Electronic Supplementary Material (ESI) for Journal of Materials Chemistry A.

Supplementary Information

Natural Wood-Based Triboelectric Nanogenerators with Highly Fire-Safety for Energy Harvesting toward Intelligent Building

Bo Tang, Ze-Peng Deng, Jia-Min Wu, Yu-Yao Zhao, Qiang-Wu Tan, Fei Song*, Xiu-Li Wang*, Yu-Zhong Wang

The Collaborative Innovation Center for Eco-Friendly and Fire-Safety Polymeric Materials (MoE), National Engineering Laboratory of Eco-Friendly Polymeric Materials (Sichuan), State Key Laboratory of Polymer Materials Engineering, College of Chemistry, Sichuan University, Chengdu, 610064, China.

* Corresponding authors: songfei520@gmail.com; xiuliwang1@163.com

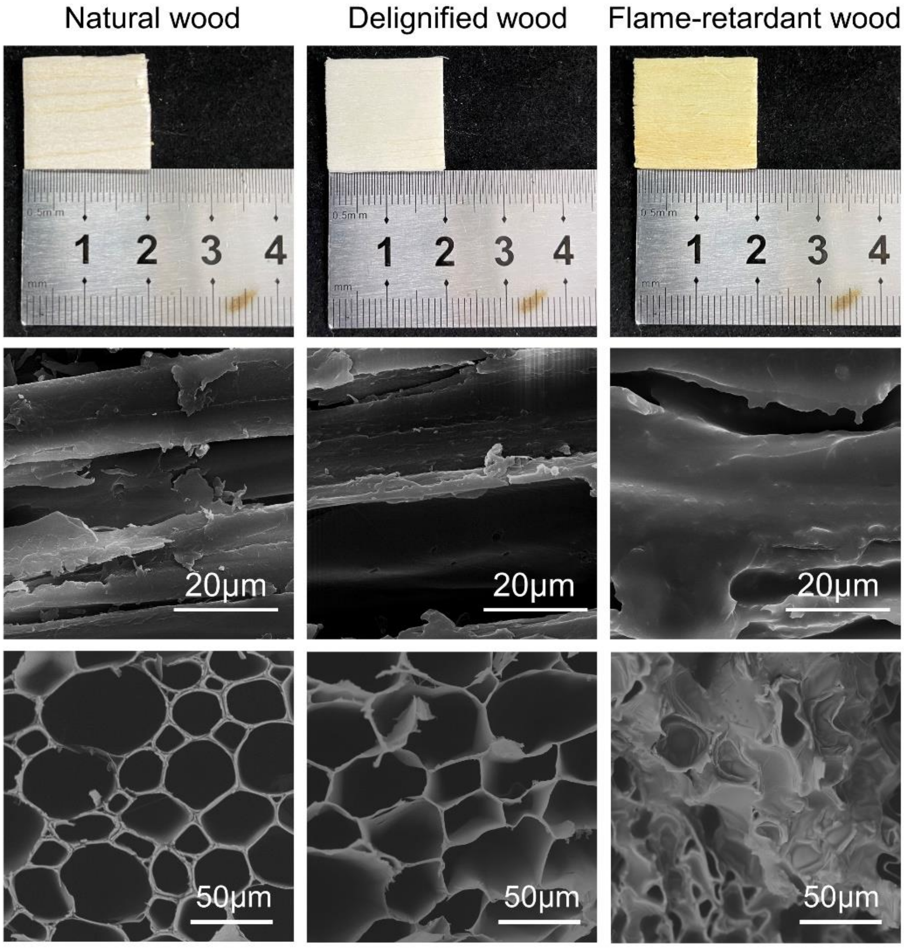

Fig. S1 Digital photographs and SEM images of natural wood, delignified wood, and flame-retardant wood.

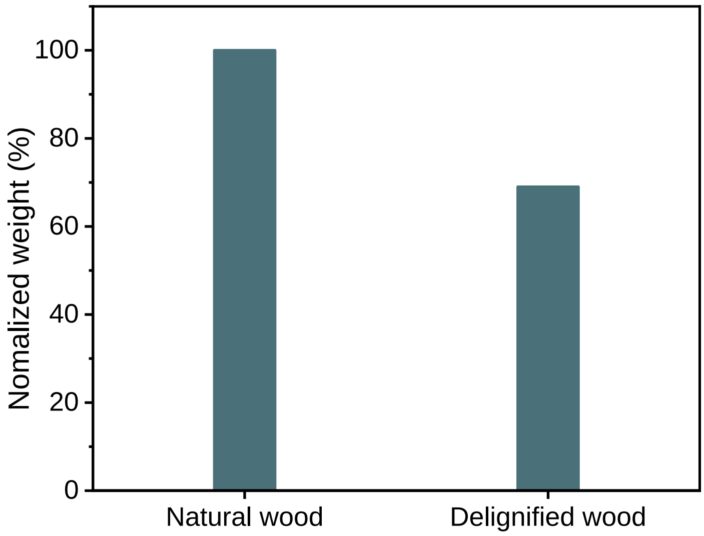

Fig. S2 Normalized weight comparison of natural wood and delignified wood.

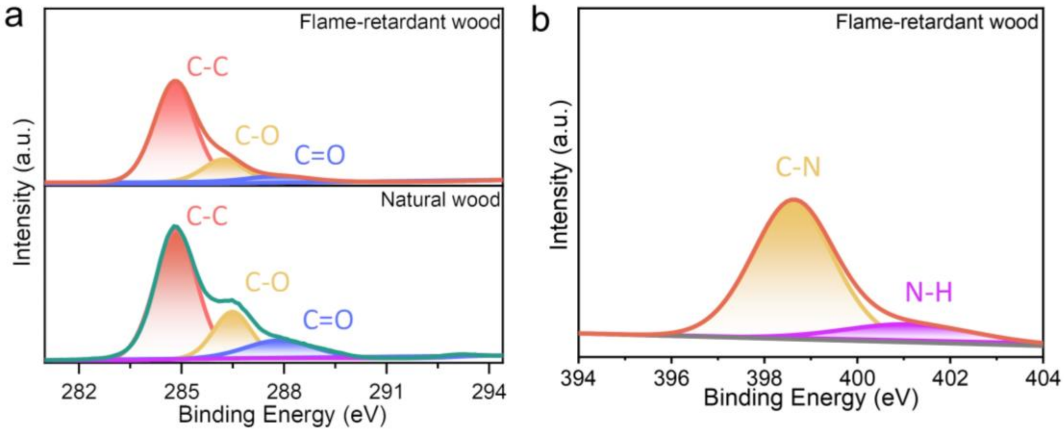

Fig. S3 (a) C-spectrum of the natural and flame-retardant wood samples. (b) N-spectrum of flame-retardant wood.

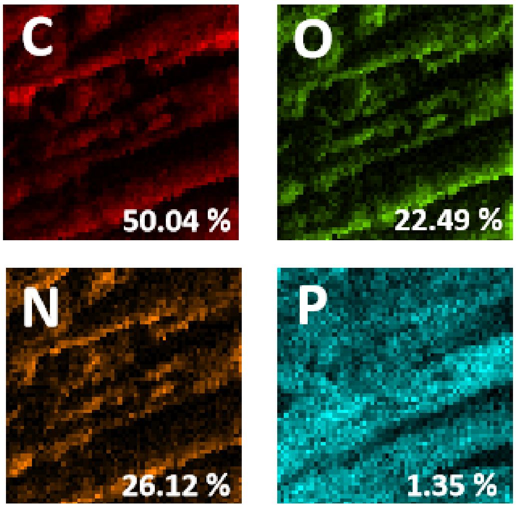

Fig. S4 EDX mapping of the flame-retardant wood.

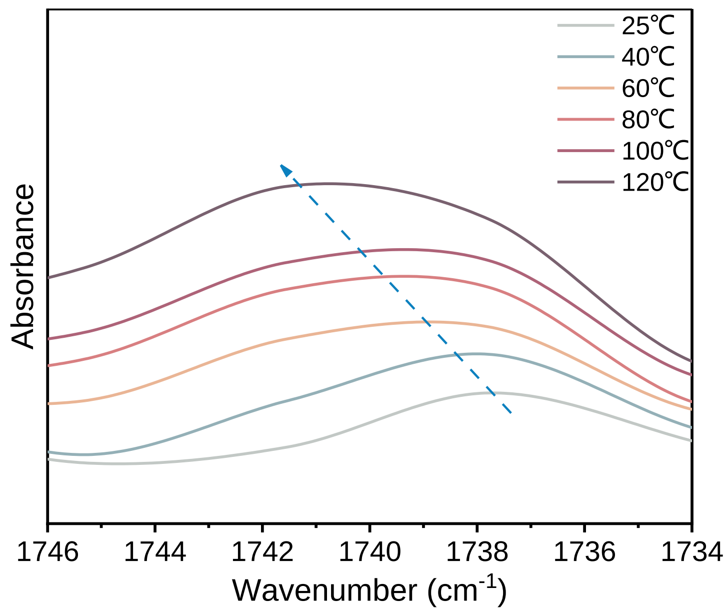

Fig. S5 In situ FTIR spectra of flame-retardant wood recorded ranging the temperature from 25 to 120 °C.

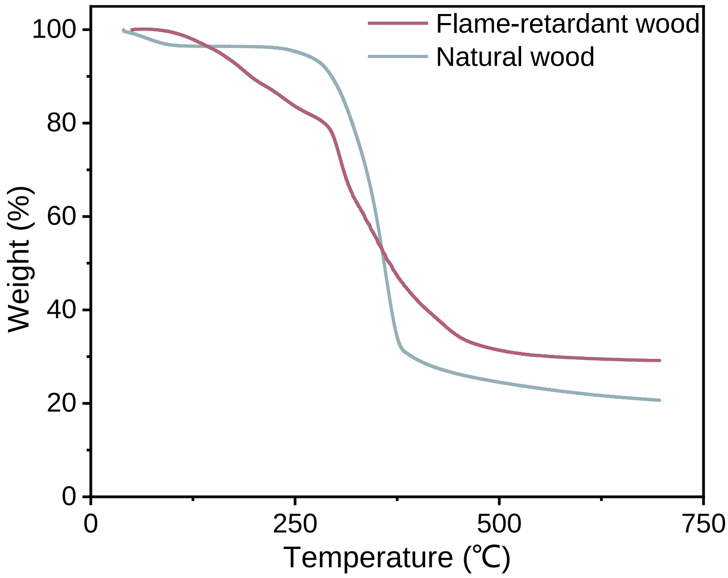

Fig. S6 TGA curves of natural wood and flame-retardant wood under N_2 atmosphere.

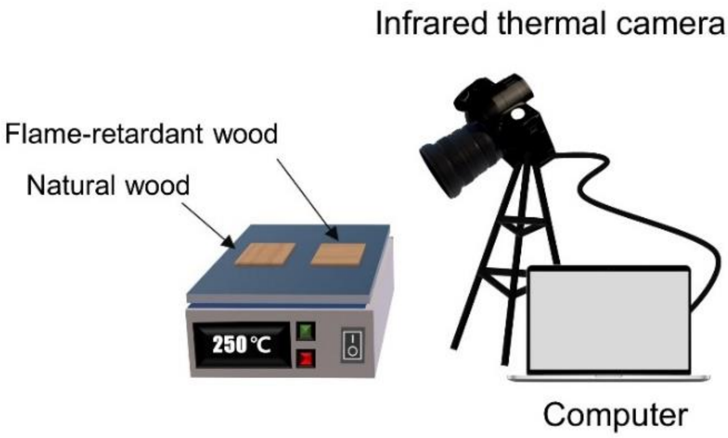

Fig. S7 Schematic diagram of the thermal insulation test for the wood samples on a 250 ℃ hot plate.

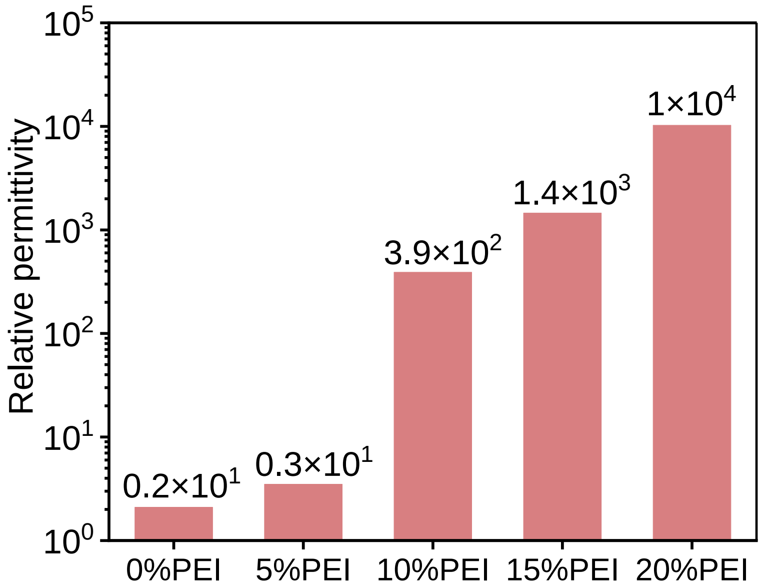

Fig. S8 Relative permittivity of flame-retardant wood at a frequency of 1000 KHz.

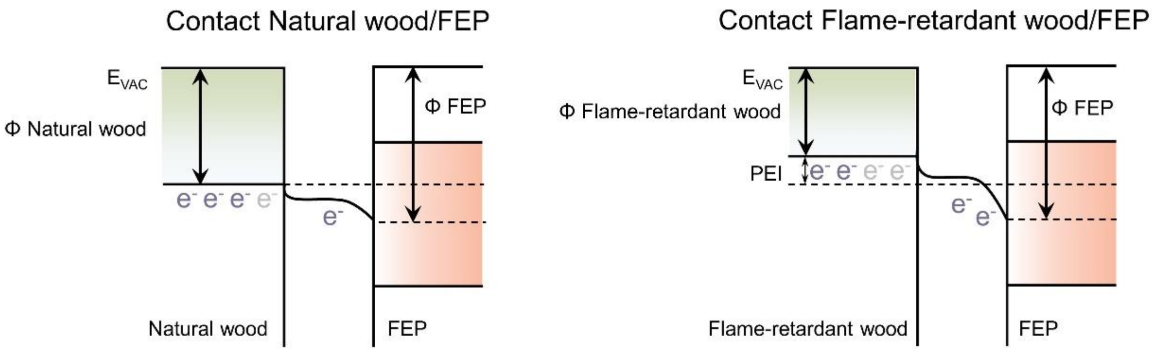

Fig. S9 Energy band diagram of Natural wood and Flame-retardant wood during contact electrification with FEP.

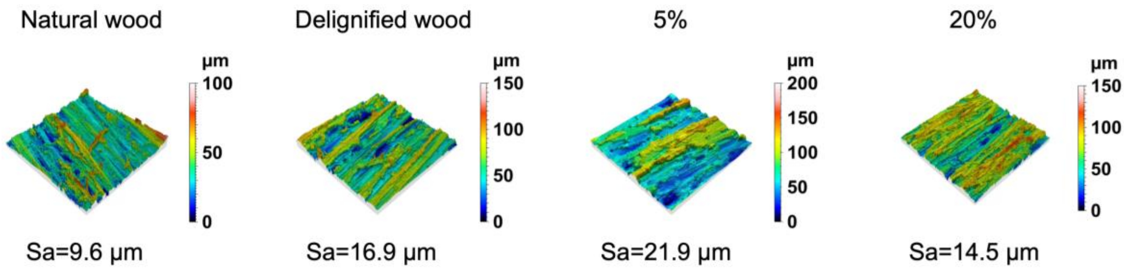

Fig. S10 3D surface profiling images of natural wood, delignified wood and flame-retardant woods.

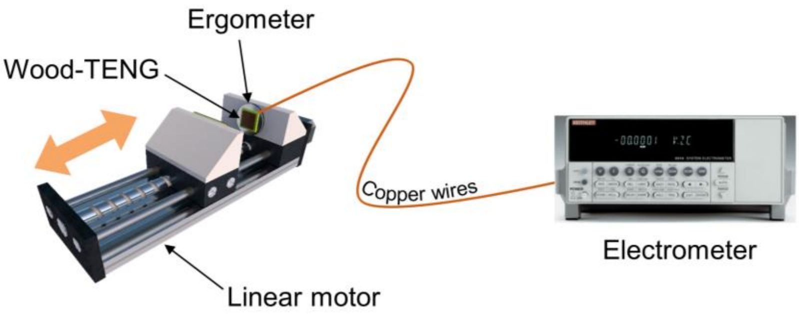

Fig. S11 The schematic diagram of the experimental platform.

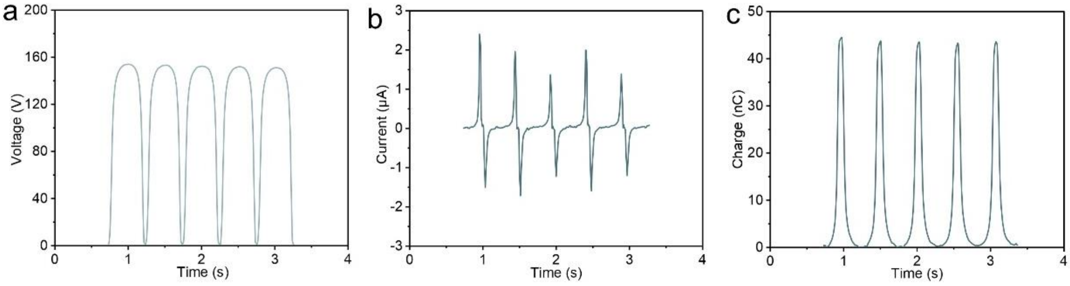

Fig. S12 (a) Open circuit voltage, **(b)** short-circuit currents, and **(c)** transferred charge of the FW-TENG prepared at the PEI concentration of 25 wt%.

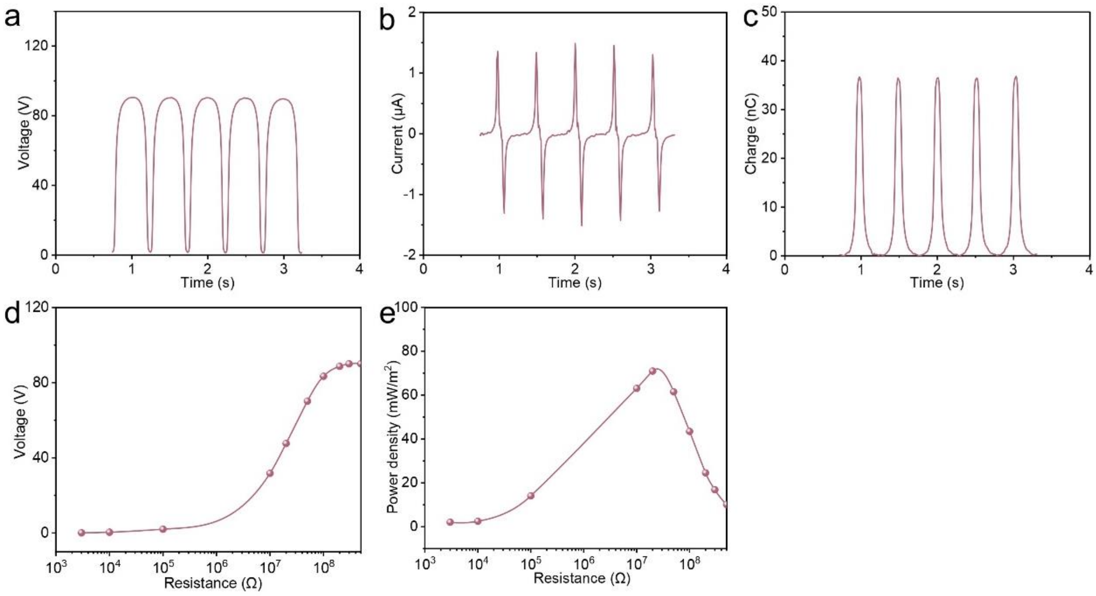

Fig. S13 Output performance of the delignified wood based TENG. (a) Open circuit voltage, **(b)** short-circuit currents, and **(c)** transferred charge of the delignified wood-based TENG. **(d)** Output voltages and **(e)** corresponding peak power density of the delignified wood-based TENG under different external load resistances.

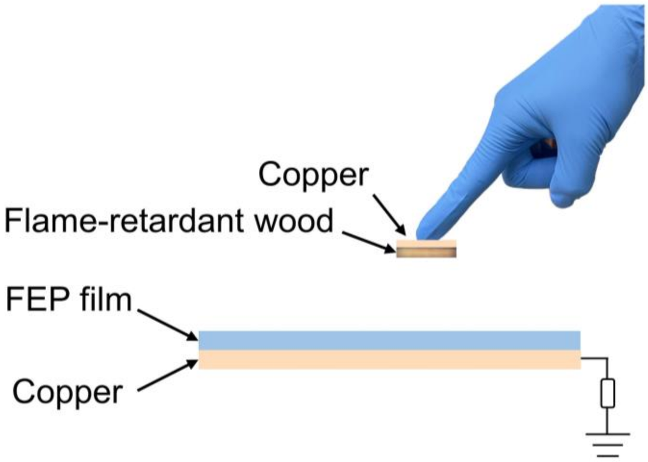

Fig. S14 Schematic illustration of the TENG as a pressure sensor.

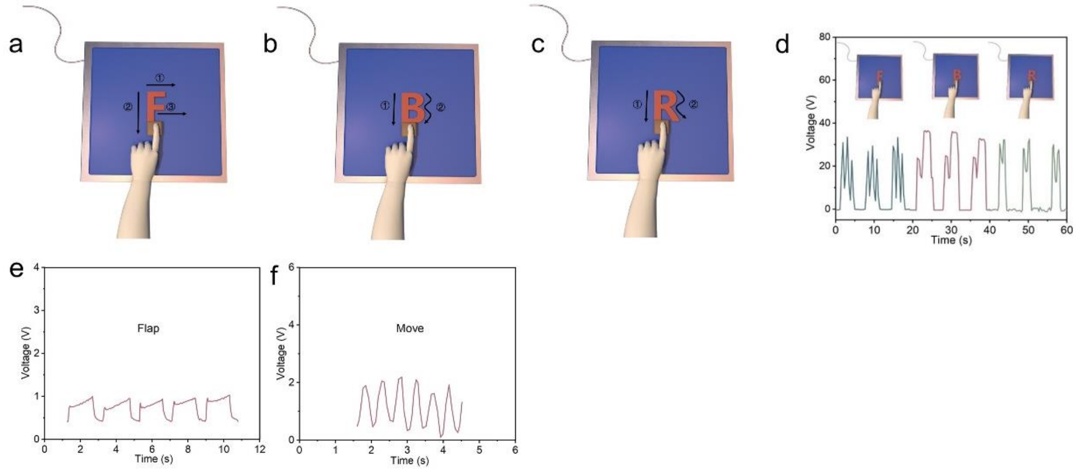

Fig. S15 (a-c) The trajectories and **(d)** voltage responses induced by writing different characters: “F” “B”, and “R”. Voltage responses induced by **(e)** flap and **(f)** move of a finger.

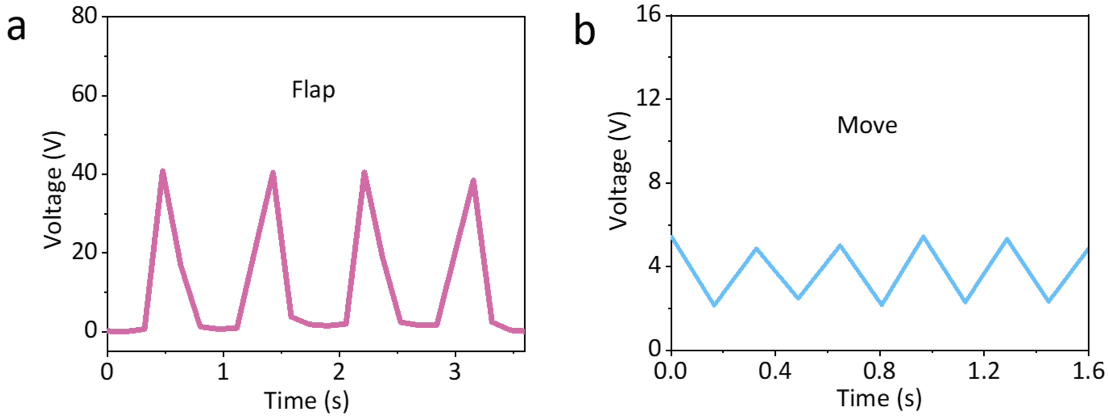

Fig. S16 Voltage responses induced by **(a)** flap and **(b)** move.

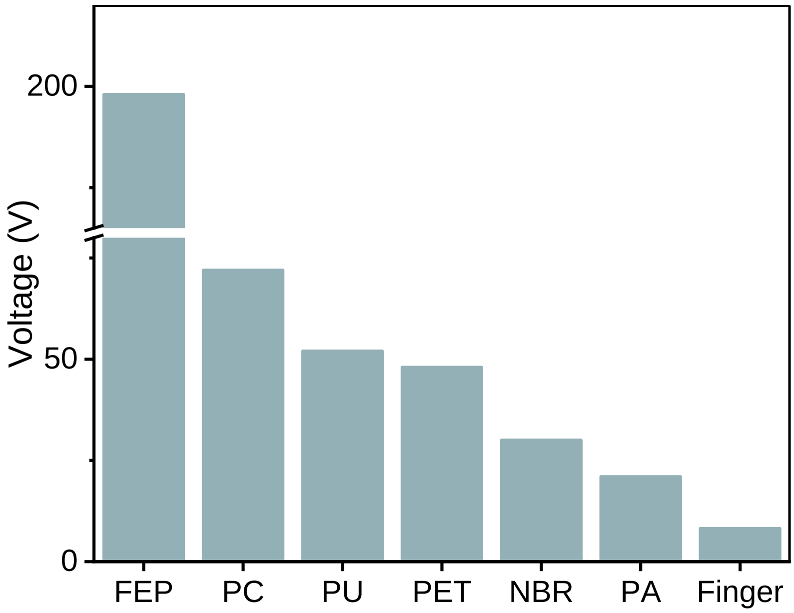

Fig. S17 Voltages of the FW-TENG in response to different contact materials.

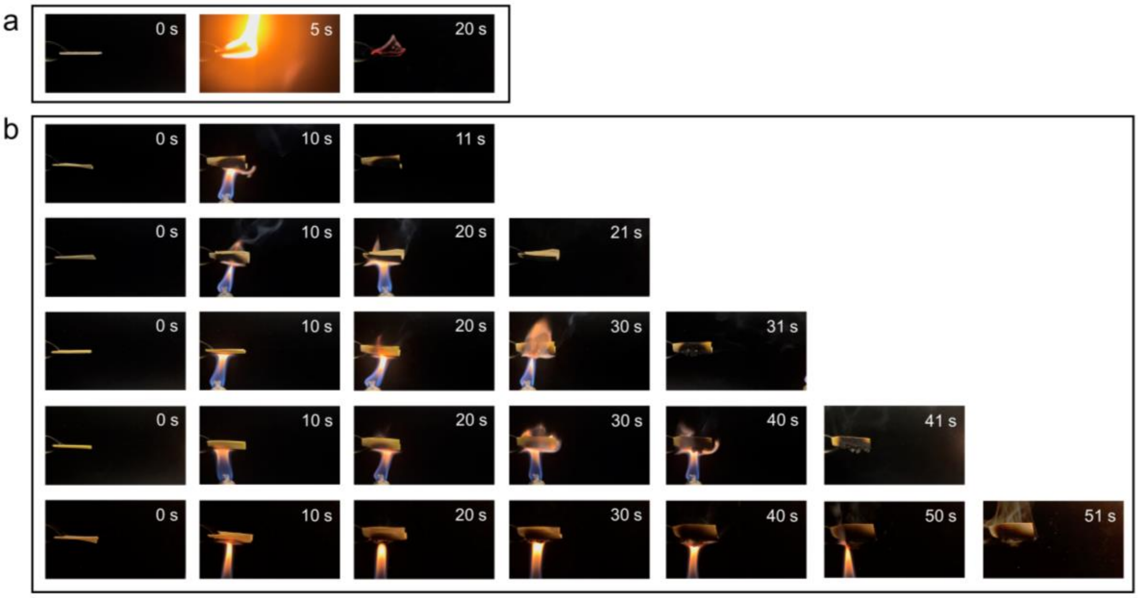

Fig. S18 Horizontal burning test of **(a)** natural wood for 5 s and **(b)** flame-retardant wood for 10 s, 20 s, 30 s, 40 s and 50 s.

Fig. S19 Vertical burning test of **(a)** natural wood for 5 s and **(b)** flame-retardant wood for 10 s, 20 s, 30 s, 40 s and 50 s.

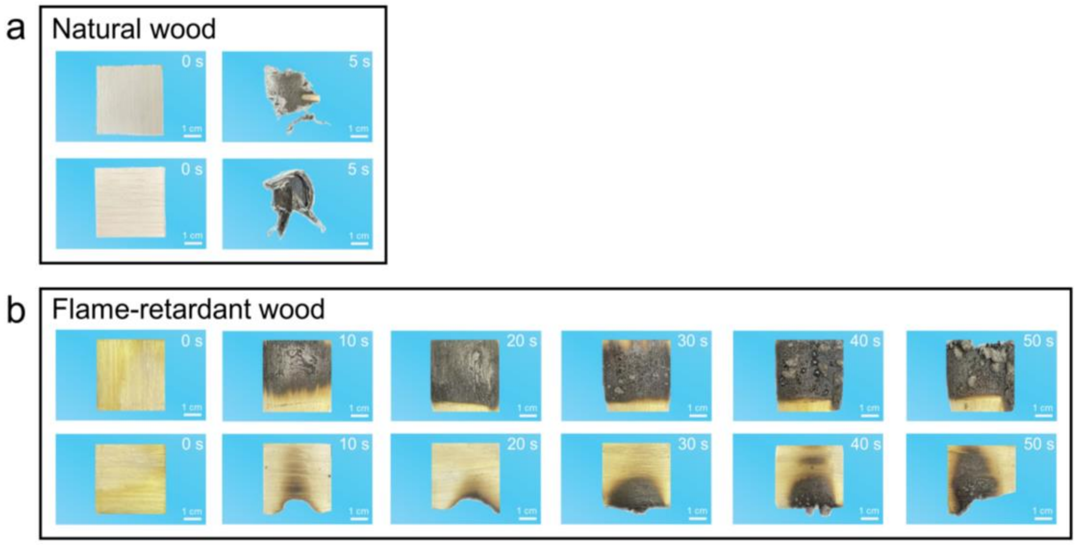

Fig. S20 Photographs of **(a)** natural wood and **(b)** flame-retardant wood after burning test.

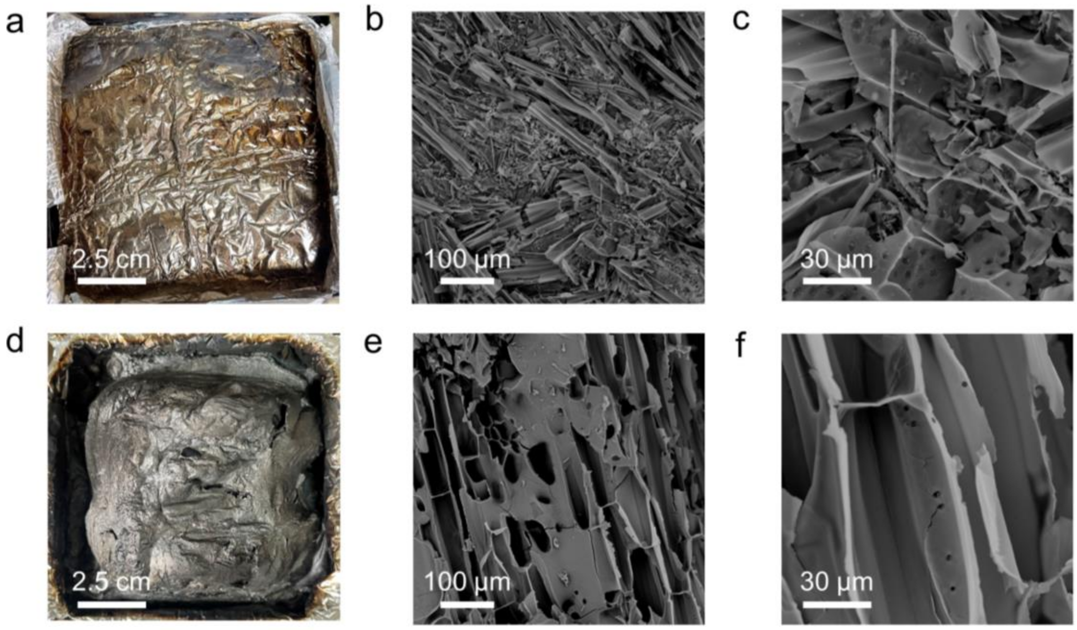

Fig. S21 Digital photographs and SEM images of **(a-c)** natural and **(d-f)** flame-retardant wood after cone calorimeter test.

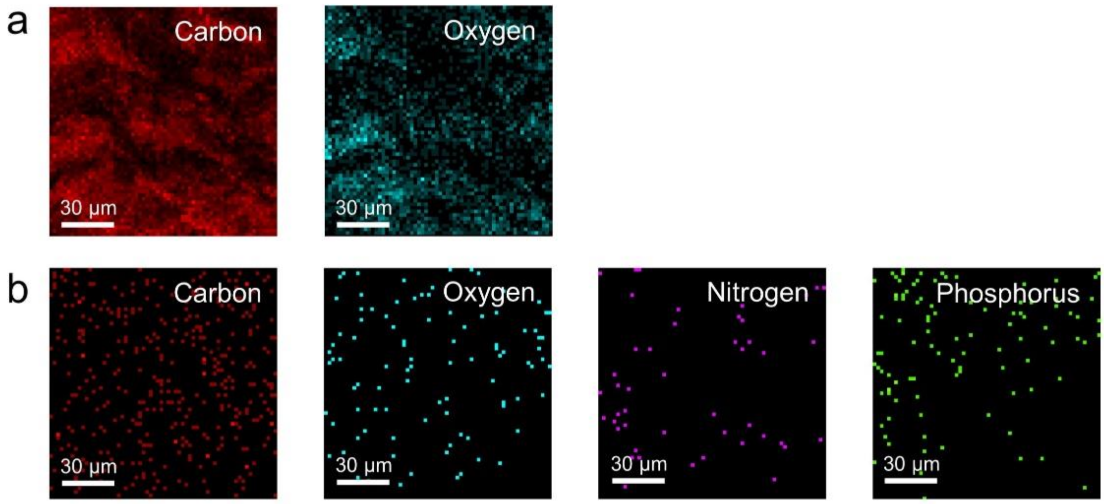

Fig. S22 EDX mapping of the **(a)** natural and **(b)** flame-retardant wood after cone calorimeter test.

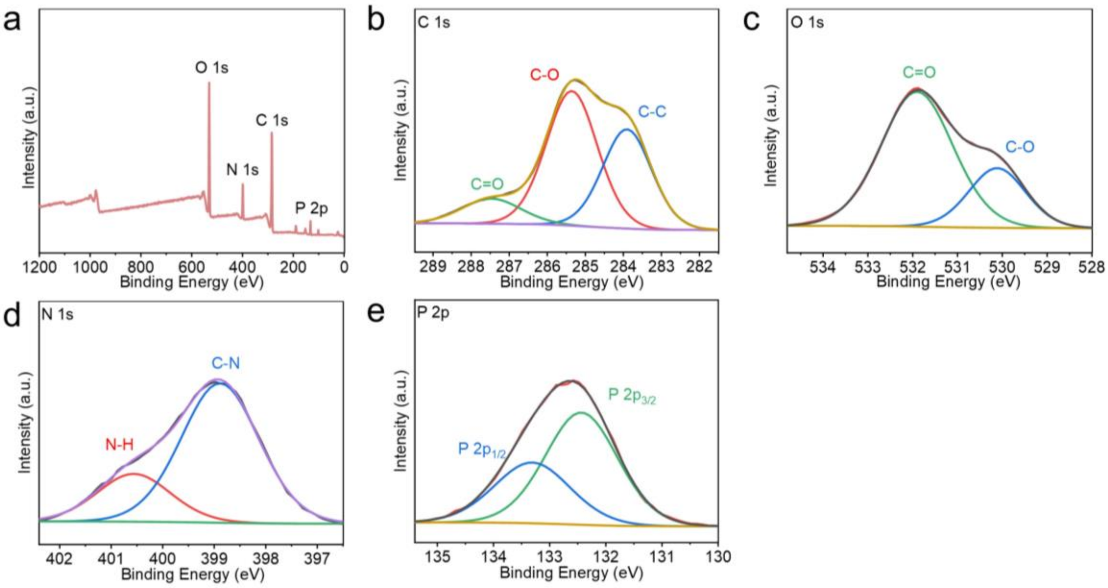

Fig. S23 XPS spectra of the flame-retardant wood after cone calorimeter test.

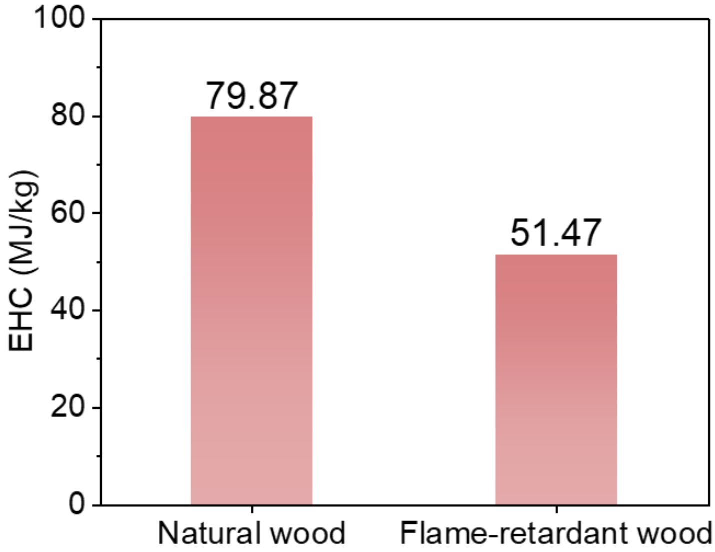

Fig. S24 Comparison of the EHC between natural and flame-retardant wood.

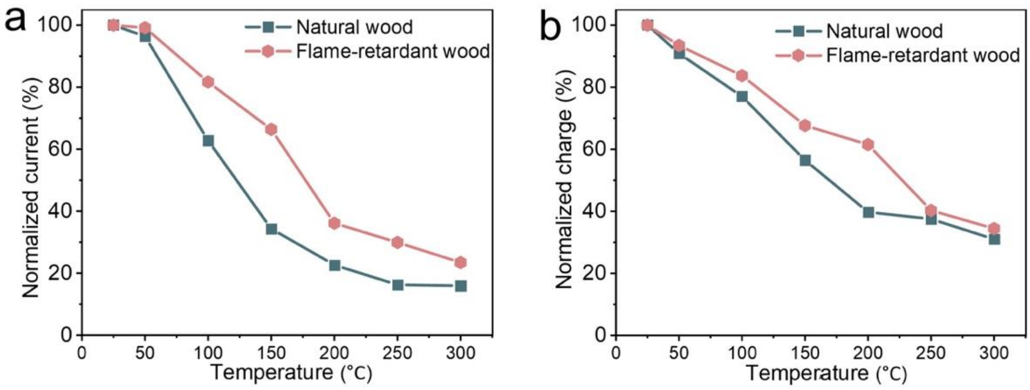

Fig. S25 Normalized **(a)** current and **(b)** charge of the TENGs fabricated with natural wood and flame-retardant wood under different temperatures.

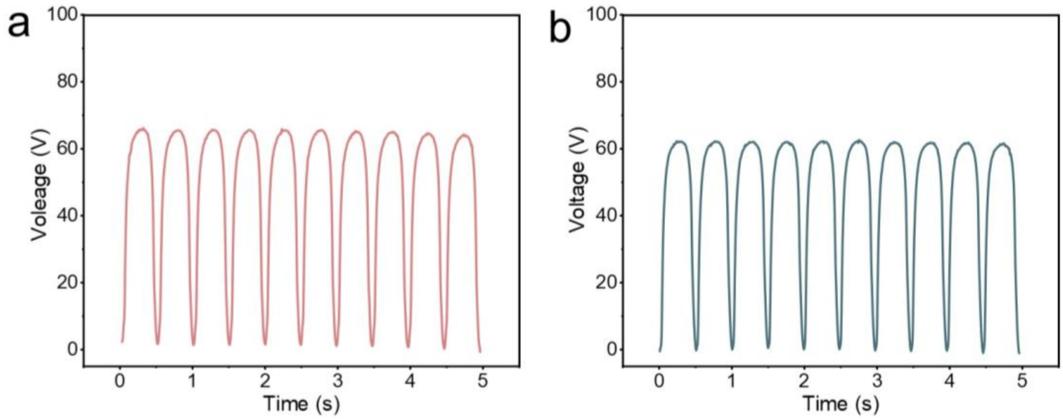

Fig. S26 Voltage output of FW-TENGs after **(a)** burning horizontally and **(b)** burning vertically for 50 s.

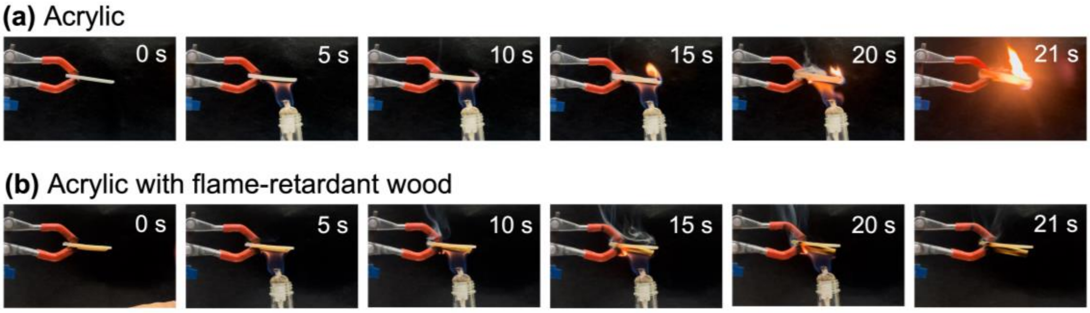

Fig. S27 Horizontal burning test of **(a)** acrylic and **(b)** acrylic with flame-retardant wood.

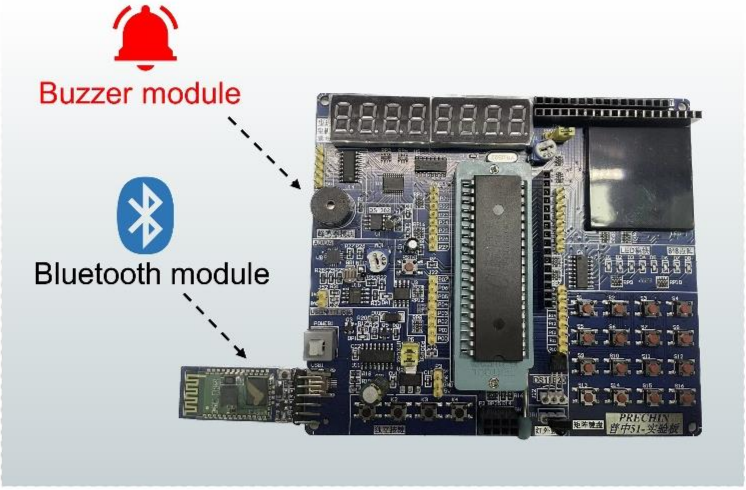

Fig. S28 Photograph of the microcontroller, buzzer module and Bluetooth module.

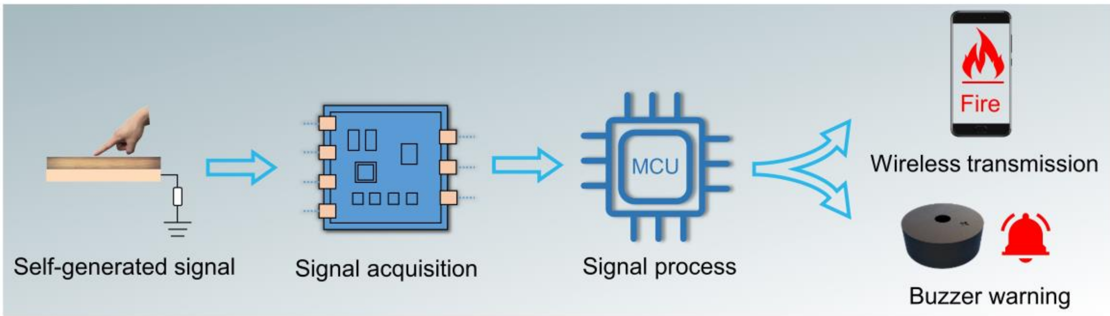

Fig. S29 The operation mechanism of the self-powered wireless fire monitoring system.

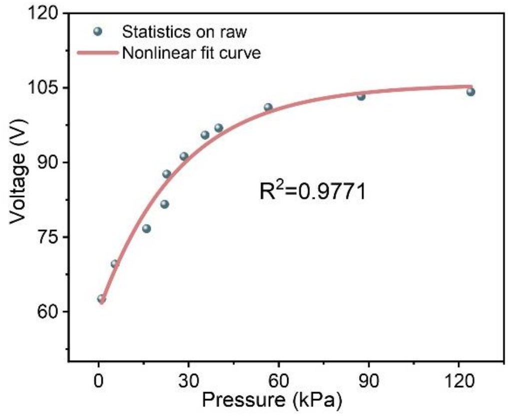

Fig. S30 Relationship between voltage and pressure.

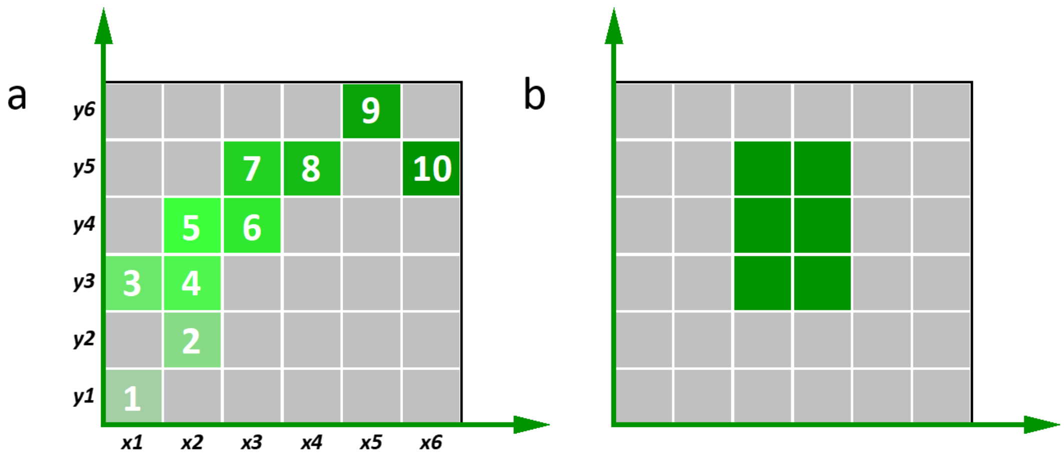

Fig. S31 Path display of walking (a) and falling (b) on the smart floor.

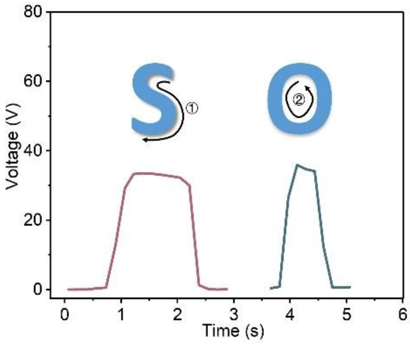

Fig. S32 The trajectories and voltage responses induced by writing characters: "S" and "O".

Table S1 Atomic concentration of natural and flame-retardant wood from XPS measurement

Samples \ Elements	C	O	N	P
	%	%	%	%
Natural wood	67.7	24.6	2.05	0.5
Flame-retardant wood	55.7	22.8	3.61	1.51

Table S2 Comparison of FW-TENG with previously reported wood-based TENGs

Voltage /V	Current/ uA	Charge Density/μC *m^{-2}	Power Density/mW /m^2	Frequency /Hz	Area/c m^2	Pressure /N	Ref
198	7.48	47	119.7	2	4*4	1	This Work
100	0.6	13.6	24.2	1	5*5	7.5	[36]
80	/	/	0.009	8	/	20	[61]
81	1.8	36	57	1	3*3	20	[28]
220	5.6	/	/	40	8*8	/	[62]
24.3	0.32	12	10.4	/	2*3.5	50	[29]
45	1.5	/	0.6	/	/	/	[63]
90.1	0.458	71.5	54.53	3	2*2	8.2	[25]
47	2.4	10	/	2	4*4	/	[64]
227	4.8	/	18.86	/	10*8	180	[30]
38	0.37	/	/	1	2*2	1	[27]
220	5.8	/	158.2	2	8*8	/	[65]

[61] D.G. Park, J.H. Hong, D.K. Choi, D.H. Kim, W.H. Jung, S.S. Yoon, K.H. Kim, S.P. An, Biocompatible and mechanically-reinforced tribopositive nanofiber mat for wearable and antifungal human kinetic-energy harvester based on wood-derived natural product, Nano Energy.96 (2022) 107091.

https://doi.org/10.1016/j.nanoen.2022.107091.

[62] C. He, W.J. Zhu, B.D. Chen, L. Xu, T. Jiang, C.B. Han, G.Q. Gu, D.C. Li, Z.L. Wang, Smart Floor with Integrated Triboelectric Nanogenerator As Energy Harvester and Motion Sensor,

ACS Appl. Mater. Interfaces. 31 (2017) 26126–26133.
https://doi.org/10.1021/acsami.7b08526.

[63] S. Bi, X. Han, Q.Q. Chen, B.H. Gao, L.H. Chen, Z.G. He, C.M. Jiang,
Ultralarge Curvature and Extreme Rapid Degradable Porous Wood Based Flexible Triboelectric Sensor for Physical Motion Monitoring, Advanced Materials Technologies. 8 (2023) 2201066.
https://doi.org/10.1002/admt.202201066

[64] C.C. Cai, J.L. Mo, Y.X. Lu, N. Zhang, Z.Y. Wu, S.F. Wang, S.X. Nie,
Integration of a porous wood-based triboelectric nanogenerator and gas sensor for real-time wireless food-quality assessment, Nano Energy. 83 (2021) 105833.
https://doi.org/10.1016/j.nanoen.2021.105833.

[65] S.F. Hao, J.Y. Jiao, Y.D. Chen, Z.L. Wang, X. Cao,
Natural wood-based triboelectric nanogenerator as self-powered sensing for smart homes and floors, Nano Energy. 75 (2020) 104957.
https://doi.org/10.1016/j.nanoen.2020.104957